Actuator Grouping Optimization Method of Antenna Reflector Based-on Ant Colony Algorithm

Yan Du[1(✉)], Songjing Ma[2], Tao Ma[3], Xiangshuai Song[2], and Jiayou Zhang[2]

[1] Institute of Telecommunication and Navigation Satellites, China Academic of Space Technology, Beijing 100094, China
duyan1120@163.com
[2] College of Aerospace and Civil Engineering, Harbin Engineering University, Harbin 150001, China
[3] Beijing Spacecraft Co., Ltd, Beijing 100094, China

Abstract. This paper aims to propose an actuator grouping optimization method for active shape control of an antenna reflector. An influence coefficient matrix (ICM) model of the reflector system is firstly derived using the finite element method. Then, the out-of-plane displacements caused by a determined supply voltage are given using ICM and actuator grouping matrix. A hybrid optimization method is proposed to obtain the optimal actuator group and power supply voltage, to significantly improve the shape control performance. The main feature of this method is to use the ant colony algorithm and least square method to optimize actuator grouping and power supply voltage step by step. Finally, numerical simulations are presented to verify the effectiveness of the proposed method. The results indicate that the proposed method is easy to fall into a local optimum, however, the shape precision using two power supplies can still be improved by more than 97%. It significantly reduces the scale and cost of the control system and demonstrates the proposed effectiveness. The computation time is shortened greatly thanks to the fast convergence rate, which has an obvious advantage in solving the optimization problem.

Keywords: Antenna reflector · Active shape control · Grouping optimization · Ant colony algorithm · Least-squares method

1 Introduction

The missions like earth observation and deep space exploration are promoting the ability demands of satellite antenna, while the gain of an antenna is depending on its antenna radius and shape precision. As a result, the difficulty of shape control for giant antennas will become more significant than in traditional [1, 2]. The shape precision of an antenna reflector is usually evaluated in accordance with the Root Mean Square(RMS) error, which can be improved by shape control using actuators [3, 4]. If the actuators are powered independently, the weight and cost of the control system would be significantly

Y. Wang et al. (Eds.): ICSINC 2022, LNEE 996, pp. 113–121, 2023.
https://doi.org/10.1007/978-981-19-9968-0_14

increased. Multiple actuators are driven using less power supply is one of the technical ways to solve the above problems [5].

A feasible design scheme using less power supply to drive multiple actuators is to connect multiple actuators to the power supplies in parallel. And then, the matching relationship between actuators and power supplies, which is the actuator group, can be adjusted by the switch. Obviously, the optimal actuator group and power supply voltage must be determined to ensure shape control performance. In the published literature, there are few studies on shape and vibration control using a limited number of power supplies. The vibration control performance is improved using less power supply in literature [6] and [7]. A global elimination method to minimize RMS error is proposed to obtain the optimal actuator group and power supply voltage [8]. An electrode grouping optimization approach is developed considering some constraints, including RMS error, stress, and voltage for an electrostatic forming membrane reflector [9].

In this paper, a hybrid optimization algorithm using the Ant Colony (AC) and Least-Squares (LS) is developed to optimize the actuator grouping and the power supply voltage, to improve shape control performance for an antenna reflector. In Sect. 2, the grid reflector is described, and the analytical model of the reflector is established using the finite element method. Then out-of-plane displacement is derived. In Sect. 3, the optimization model and process are presented. In Sect. 4, the feasibility of the proposed optimization method is verified through numerical simulation. Finally, the brief conclusion is presented in Sect. 5.

2 Reflector System Modeling

2.1 Description of the Grid Reflector

The solid grid reflector is a hexagonal paraboloid with a diameter of 1 m and a focal length of 2.1 m, consisting of a reflector surface, U-shaped ribs, and piezoelectric (PZT) actuators, as shown in Fig. 1. The base structure is consisting of the reflector surface and the U-shaped ribs, which is a multilayer carbon fiber laminated plate structure. The PZT actuator is embedded in the U-shaped rib and drives base structure deformation

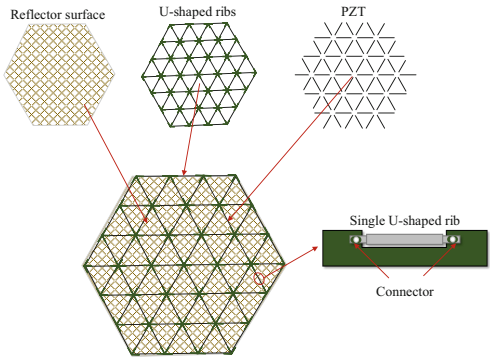

Fig. 1. Scheme of a grid reflector structure.

using the converse piezoelectricity. Each U-shaped rib is embedded with a PZT actuator through a mechanical connector. Then, 72 PZT actuators are mounted on the back side of the reflector.

2.2 Finite Element Model

The finite element method is used to establish the mechanical model of the reflector. The shell element with 4-node is used for the base structure. The dynamics equation can be derived from Hamilton's principle

$$\boldsymbol{M}_{uu}^{h}\ddot{\boldsymbol{u}}^{h} + \boldsymbol{K}_{uu}^{h}\boldsymbol{u}^{h} = \boldsymbol{f}^{h} \tag{1}$$

where matrix $\boldsymbol{M}_{uu}^{h}$ and matrix $\boldsymbol{K}_{uu}^{h}$ represent the mass and stiffness respectively, $\boldsymbol{u}^{h}$ denotes the nodal displacement vector, $\boldsymbol{f}^{h}$ represents the nodal load vector, and the superscript h represents the base structure element.

The PZT actuator is formed by stacking the piezoelectric wafer, and only the deformation along the axial direction is considered. Then, the bar element with a 2-node is used for the PZT actuator. Based on the piezoelectric constitutive Eq. (2) and Hamilton's principle,

$$\begin{aligned} T_3 &= c_{33}S_3 - e_{33}E_3 \\ D_3 &= e_{33}S_3 + \varepsilon_{33}E_3 \end{aligned} \tag{2}$$

where T_3 and S_3 are the axial stress and strain, respectively, D_3 and E_3 characterized as the axial electric displacement vector and electric field strength, respectively, c_{33} is the elastic coefficient of piezoelectric material, e_{33} indicates the piezoelectric strain constant, ε_{33} represents the vacuum dielectric constant.

The dynamics equation of the PZT actuator can be illustrated as follows

$$\boldsymbol{M}_{uu}^{p}\ddot{\boldsymbol{u}}^{p} + \boldsymbol{K}_{uu}^{p}\boldsymbol{u}^{p} = \boldsymbol{f}^{p} - \boldsymbol{f}_{v}^{p} \tag{3}$$

where $\boldsymbol{M}_{uu}^{p}$ and $\boldsymbol{K}_{uu}^{p}$ are the mass matrix and stiffness matrix, respectively, $\boldsymbol{u}^{p}$ denotes the nodal displacement vector, $\boldsymbol{f}^{p}$ represents the nodal load vector, $\boldsymbol{f}_{v}^{p}$ is the driving force, and the superscript p represents the PZT element.

All elements are transferred to the global coordinate system and finally assembled; the dynamics equation of the reflector can be illustrated as

$$\overline{\boldsymbol{M}}\ddot{\boldsymbol{u}} + \overline{\boldsymbol{K}}\boldsymbol{u} = \boldsymbol{f} - \overline{\boldsymbol{B}}\boldsymbol{v} \tag{4}$$

where, $\overline{\boldsymbol{M}}$ and $\overline{\boldsymbol{K}}$ demonstrate the mass matrix and stiffness matrix of the reflector structure, respectively, $\boldsymbol{f}$ means the nodal external force vector, $\overline{\boldsymbol{B}}$ means the actuator input matrix, and $\boldsymbol{v}$ is the actuator voltage vector.

The primary of the research is shape control. Thus, the influence of structural vibration is ignored, and the statics equation can be illustrated as follows

$$\overline{\boldsymbol{K}}\boldsymbol{u} = \boldsymbol{f} - \overline{\boldsymbol{B}}\boldsymbol{v} \tag{5}$$

2.3 Out-of-Plane Displacement Description

It can be seen from Eq. (5) that the deflection of the reflector is caused by the load $\boldsymbol{f}$ and actuator force $\overline{\boldsymbol{B}}\boldsymbol{v}$. Because the significant external load is the space thermal radiation load, its change is slow. When the actuator voltage changes, $\boldsymbol{f}$ is assumed to be constant. The difference in the displacement of the reflector surface caused by a change in voltage can be illustrated as follows

$$\Delta \boldsymbol{u} = \overline{\boldsymbol{K}}^{-1}\overline{\boldsymbol{B}}\Delta \boldsymbol{v} \tag{6}$$

The RMS error in the out-of-plane displacements of sensor points on the reflector surface is often used to assess the shape accuracy, and the out-of-plane displacements can be expressed as [10]

$$\Delta \overline{\boldsymbol{u}} = \boldsymbol{B}_v \Delta \boldsymbol{v} \tag{7}$$

where $\boldsymbol{B}_v = \boldsymbol{C}\overline{\boldsymbol{K}}^{-1}\overline{\boldsymbol{B}}$ is the influence coefficient matrix, and $\boldsymbol{C}$ is the position matrix.

Supposed that the number of power supplies is limited, multiple actuators are connected with different power supplies in parallel, and toggle switches are used to adjust the matching relationship between actuators and power supplies. The mapping between the supply voltage and the actuator voltage can be described by the grouping matrix $\boldsymbol{H}$, which can be expressed as

$$\boldsymbol{v} = \boldsymbol{H}\boldsymbol{v}_p \tag{8}$$

where $\boldsymbol{v}$ is the voltage vector used by actuators and the $\boldsymbol{v}_p$ is the output voltage vector from the battery, $\boldsymbol{H}$ is a matrix that separates actuators into groups, its elements are 0 or 1, and matrix $\boldsymbol{H}$ consists of m row p column, m means the number of the actuator, and p denotes the number of power supply. The column position of the 1 represents that the actuator is connected to the corresponding power supply, and each row of the matrix $\boldsymbol{H}$ has only one 1, as shown in Fig. 2.

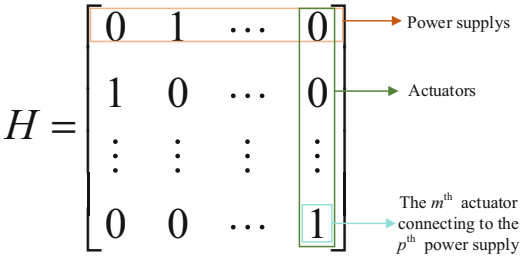

Fig. 2. Actuator grouping matrix.

When Eq. (7) is substituted into Eq. (8), the out-of-plane displacement caused by a change in the supply voltage can be given by

$$\Delta \overline{\boldsymbol{u}} = \boldsymbol{B}_v \boldsymbol{H} \Delta \boldsymbol{v}_p \tag{9}$$

3 Optimization Model and Processes

The shape control performance using a limited number of power supplies is affected by the actuator grouping and the supply voltage. A hybrid optimization method using the AC algorithm and LS method is present to determine the optimal actuator grouping and the supply voltage. The optimization configuration is described in the following, including the objective function, design variables, constraints, and optimization process.

(1) Objective function
The objective function substantiates set as the RMS error of the reflector surface, which represents shape precision. The RMS error can be illustrated as follows

$$\delta = \sqrt{\frac{1}{N}(\Delta \boldsymbol{u} - \Delta \boldsymbol{u}_d)^{\mathrm{T}}(\Delta \boldsymbol{u} - \Delta \boldsymbol{u}_d)} \tag{10}$$

where δ is the RMS error, $\Delta \boldsymbol{u}_d$ is the desired displacement.

(2) Design variable
The design variable includes the actuator grouping and the supply voltage. The column position of 1 in the $\boldsymbol{H}$ represents the grouping of actuators. Thus, the design variable can be illustrated as

$$\begin{cases} \boldsymbol{\kappa} = \left[\kappa_1 \ \kappa_2 \ \ldots \ \kappa_m\right]^{\mathrm{T}} \\ \boldsymbol{v}_p = \left[v_1 \ v_2 \ \ldots \ v_p\right]^{\mathrm{T}} \end{cases} \tag{11}$$

where $\boldsymbol{\kappa}$ is an m-dimension column vector, κ_m is the column position of the 1 in m row of the $\boldsymbol{H}$.

(3) Constraint condition
κ_m is the column position of the 1, which is a positive integer not exceeding p. The actuator voltage should satisfy the voltage constraint to avoid damaging the piezoelectric material. Thus, the constraint conditions can be expressed as

$$\begin{cases} \boldsymbol{0} < \boldsymbol{\kappa} \le p\boldsymbol{O}_{ne} (\boldsymbol{\kappa} \in \mathbb{Z}) \\ \boldsymbol{v}^c_{\min} \le \boldsymbol{v}_p \le \boldsymbol{v}^c_{\max} \end{cases} \tag{12}$$

where $\boldsymbol{O}_{ne}$ is an m- dimension vector consisting of one. $\boldsymbol{v}_{\min}$ and $\boldsymbol{v}_{\max}$ characterized as the minimum and maximum voltage of the power supply, respectively.

(4) Optimization process
A hybrid optimization method is proposed to solve this optimization problem. An AC algorithm is used to optimize the actuator grouping, and then the LS method is used to optimize the power supply voltage [11]. As shown in Fig. 3, the optimization process is summarized as follows.

1) Initialize the parameters.
2) Randomly choose a direction to move to the next node.

3) Locally update pheromone strength which is given by

$$\tau_{ij} = (1-\rho)\tau_{ij} + \rho\tau_0 \tag{13}$$

where τ_0 means the initial value of pheromone intensity, τ_{ij} denotes the pheromone intensity of the ij-th node, ρ is a constant between 0 and 1.

4) Determine whether ants have completed the iteration. The process is continued if the iteration is completed; otherwise, the process is continued from step 3.
5) The grouping matrix $\boldsymbol{H}$ is generated, and using the LS method is effective to solve the optimal power supplies.
6) After calculating the RMS error, the optimal solution is selected for updating the global pheromone. The updated format is as follows

$$\tau_{ij} = (1-\lambda)\tau_{ij} + \lambda\Delta\tau_{ij} \tag{14}$$

$$\Delta\tau_{ij} = \begin{cases} Q/L(i,j) \text{ on the path} \\ 0 \qquad \text{otherwise} \end{cases} \tag{15}$$

where λ is the pheromone volatility coefficient, $\Delta\tau_{ij}$ denotes the increase of the pheromone intensity, Q is a proportional coefficient, and L represents the optimal RMS value.

7) Determine whether the convergence condition is met. The optimization terminates if the stop condition is completed; otherwise, the process is continued from step 3.

4 Results and Discussions

In this part, there are some results of the optimization method presented and discussed. The ply orientations are $(0°/45°/-45°/90°)_s$, and the thickness of each layer is 0.1 mm. There are the material properties of every carbon fiber layer and actuator in Table 1. The

Table 1. Performance of each carbon fiber layer and actuator.

Parameters	Values	
	Carbon fiber layer	Actuator
Young's modulus (GPa)	$E_x = 263, E_y = E_z = 11$	$E = 26.5$
Shear modulus (GPa)	$G_{xy} = G_{xz} = 5.28, G_{yz} = 4.23$	
Poison's ratio	$\mu_{xy} = \mu_{xz} = \mu_{yz} = 0.3$	$\mu = 0.3$
Density (kg/m^3)	$\rho = 1850$	$\rho_p = 8000$
Cross-section diameter (m)		$d = 0.0012$
Length (m)		$L = 0.1$
Coefficient of thermal expansion (/°C)	$\alpha_x = -0.1e^{-6}$ $\alpha_y = 38.1e^{-6}$	α_p=$4e^{-6}$
Actuator voltage range (V)		−100~100

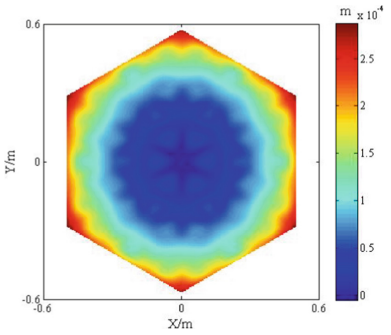

Fig. 3. Initial out-of-plane deformation distributions.

thermal distortions caused by the bulk temperature shift and a temperature gradient are used as initial errors, as the information shown in Fig. 3. The error of this initial RMS is 121.8 μm.

The number of power supply is set as 2. All numerical simulations are performed on a computer with a Core i5-9400 CPU, 2.9 GHz processors, and 16 GB of memory. The parameters of the AC are set as follows, $\rho = 0.1$, $Q = 100$. The pheromone importance $\alpha = 1$, and the heuristic function importance factor $\beta = 5$. The maximum iteration number is 300.

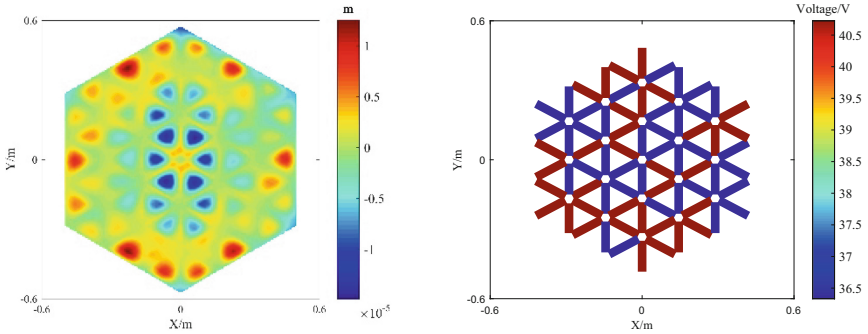

(a) (b)

Fig. 4. (a) Error distributions, (b).

Figure 4 shows the error distributions and actuator voltage distributions. The RMS error is 3.3 μm, with a reduction of 97.3%. It indicates the optimal solution tremendously reduces the weight and cost of the control system with high shape precision. The power voltages are 40.7 V and 36.3 V, respectively. The computation time consumption is 178 s, which is short enough for quasi-static shape control. Figure 5 demonstrates the curve of RMS error and calculation time as the various ant colony scale. It can be seen that the shape accuracy does not be improved significantly as the increase in ant colony size, while the computational time consumption increases. This is mainly due to the randomness of the ant colony algorithm, and it is too hard to avoid falling into the local

optimum. The primary calculation time is the LS method, which leads to a longer time consumption for the larger ant colony scale.

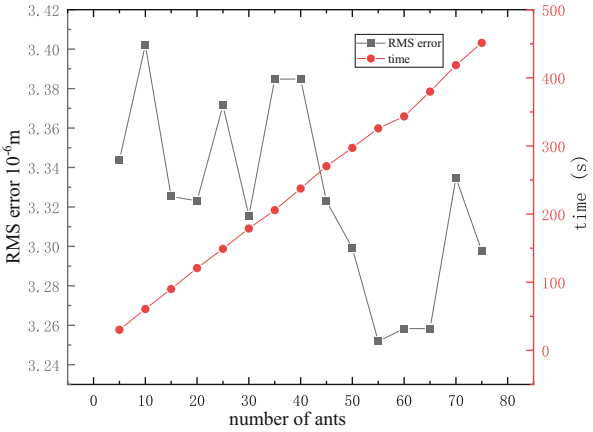

Fig. 5. RMS error and calculation time as the various in ant colony scale.

5 Conclusions

An actuator grouping optimization method of a reflector is proposed to improve shape accuracy and reduce the weight and cost of the control system. The main feature of this method is to use the ant colony algorithm and least square method to optimize actuator grouping and power supply voltage step by step. For the given thermal distortions, the effectiveness of this method is proven by massive numerical simulations. The results indicate that the shape precision using two power supplies can still be improved by more than 97%, which significantly reduces the scale and cost of the control system and demonstrates the method is highly effective. The shape accuracy does not be improved significantly as the increase in ant colony size, while the computational time consumption increases. The overall calculation time is short and acceptable, which has an obvious advantage in solving the optimization problem.

References

1. Xiaofei, M.: Development and tendency of large space deployable antenna reflector. Space Electron. Technol. **15**(02), 16–26 (2018)
2. Steeves, J., Pellegrino, S.: Ultra-thin highly deformable composite mirrors. In: 54th AIAA/ASME/ASCE/AHS/ASC Structures, Structural Dynamics, and Materials Conference 2013, Boston, MA, United States (2013)
3. Badford, S.C., Agens, G.S., Ohara, C.M., Green, J.J., Shi, F., Zhou, H., et al.: Controlling wavefront in lightweight reflector systems using piezocomposite actuator array. In: 54th AIAA/ASME/ASCE/AHS/ASC Structures, Structural Dynamics, and Materials Conference 2013, Boston, MA, United States (2013)

4. Xiangshuai, S.: Research progresses and prospect of active shape control for space-borne antenna reflectors. Space Electron. Technol. **19**(01), 1–12 (2022)
5. Irschik, H.: A review on static and dynamic shape control of structures by piezoelectric actuation. Eng. Struct. **24**(1), 5–11 (2002)
6. Grewal, A., Tse, D.: Optimization of piezoelectric actuator grouping for aircraft cabin noise control. In: 41st Structures, Structural Dynamics, and Materials Conference and Exhibit 2000, Atlanta, GA, United States (2000)
7. Jamoom, M.B., Feron, E., McConley, M.W.: Optimal distributed actuator control grouping schemes. In: Proceedings of the 37th IEEE Conference on Decision and Control 1998, Tampa, FL, United States (1998)
8. Hill, J., Wang, K.W., Fang, H.: Advances of surface control methodologies for flexible space reflectors. J. Spacecraft Rock **50**(4), 816–828 (2013)
9. Zhang, Y., Gao, F., Zhang, S., Hao, J.: Electrode grouping optimization of electrostatic forming membrane reflector antennas. Aerosp. Sci. Technol. **41**, 158–166 (2015)
10. Song, X., Tan, S., Wang, E., Wu, S., Wu, Z.: Active shape control of an antenna reflector using piezoelectric actuators. J. Intell. Mater. Syst. Struct. **30**(18–19), 2733–2747 (2019)
11. Neumann, F., Witt, C.: Runtime analysis of a simple ant colony optimization algorithm. Algorithmica **54**(2), 243–255 (2009)